Carbon dioxide capture from atmospheric air using sodium hydroxide spray: Supporting Information

Joshuah K. Stolaroff David W. Keith Gregory V. Lowry

February 1, 2008

This document consists of twelve pages of text including five figures and one table in support of the manuscript "Carbon dioxide capture from atmospheric air using sodium hydroxide spray" published in Environmental Science and Technology.

Example air capture system

Figure SI1 shows an example system for carbon capture from ambient air using the most conventional technology. It combines a contactor like that described in the main text with the kraft process for caustic recovery, which has been used for decades at large scale in pulp and paper mills (*1*). The contactor absorbs CO_2 into a sodium hydroxide (NaOH) solution, forming sodium carbonate (Na_2CO_3) solution, which is then sent to the "causticizer", where the NaOH is regenerated by addition of lime (CaO) in a series of batch processes. The resulting calcium carbonate ($CaCO_3$) solid is sent to the calciner where it is heated in a kiln to regenerate the CaO, driving off the CO_2 in the process known as calcination. The CO_2 is then captured from the flue gas by conventional means (such as an amine system), compressed, and sequestered for long term storage. Alternately, the calciner may be fired with pure oxygen instead of air. The flue gas is then dried and compressed directly. The net result is that CO_2 is concentrated from atmospheric levels to those required for compression and storage. The primary inputs are energy, water, and small amounts of Na_2CO_3 and $CaCO_3$ to make up for inefficiencies in the regeneration process (*2*).

Comparison of mass-transfer models

We first assume gas-phase limitation to mass transfer, so that the flux of CO_2 to a drop surface, J_{CO_2}, is given by (*3*):

$$J_{CO_2} = k_g(C_\infty - C_s) \tag{SI1}$$

where k_g is the gas-side mass transfer coefficient, C_∞ is the CO_2 concentration in the bulk air, and C_s is the equilibrium CO_2 concentration in air at the surface of the drop, which is effectively zero for high-pH solutions such as ours. We estimate k_g with an empirical correlation in terms of the Sherwood number, *Sh*, (*4*):

$$Sh = 2 + 0.6Re^{1/2}Sc^{1/3} \text{ and } Sh = \frac{k_g d}{D_g} \tag{SI2}$$

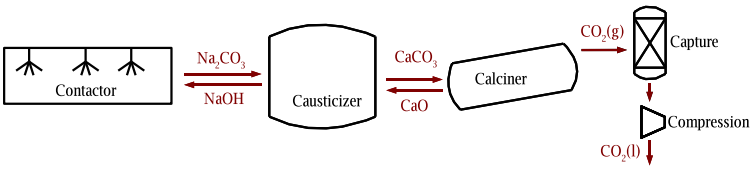

Figure SI1: Example air capture system. CO_2 from the atmosphere is absorbed into NaOH solution in the contactor. The resulting Na_2CO_3 solution is regenerated to NaOH in a series of reaction vessels by addition of CaO in the causticizer. The resulting $CaCO_3$ solids are in turn regenerated to CaO by heating in the calciner. CO_2 in the calciner flue gas is captured and compressed by conventional means.

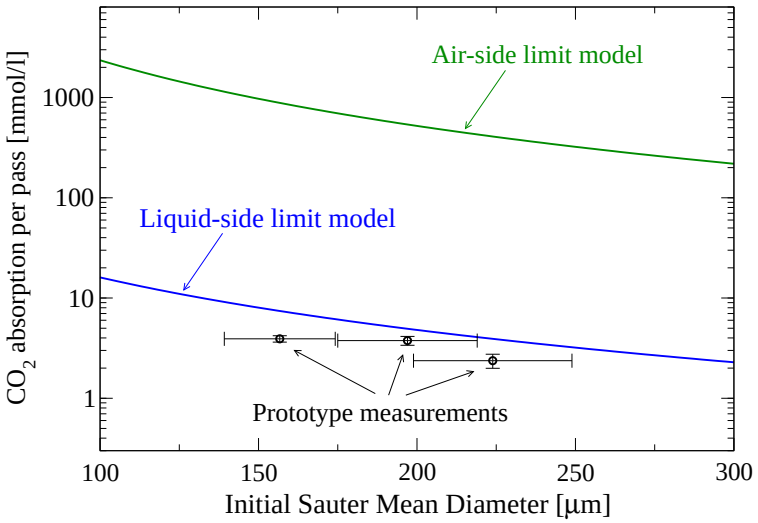

Figure SI2: Comparison of CO_2 absorption by a single falling drop predicted assuming gas-side limitation to mass transfer (upper curve) and assuming liquid-side limitation (lower curve) with comparable prototype measurements. Results indicate liquid-side resistance is limiting. Circles represent measured aggregate absorption by a spray with the indicated mean drop diameter, as inferred from nozzle manufacturer reported data for flow rate and drop size as a function of nozzle pressure. Measured nozzle pressures are shown beneath each point. Error bars represent combined subjective uncertainties and standard error of repeated measurements.

where *Re* is the Reynolds number and *Sc* is the Schmidt number for a drop falling at terminal velocity with diameter d, and D_g is the diffusion coefficient for CO_2 in air. Using *Re* and *Sc* for a drop falling at terminal velocity, $k_g$is calculated for a range of d. Multiplying J_{CO_2} by the surface area and dividing by the volume of a drop gives absorption per unit volume of solution, then multiplying by residence time, τ, gives CO_2 absorption per pass:

$$\Delta M_{pass,air} = \frac{6}{d} k_g (C_\infty - C_s).$$

Figure SI2 shows the results for this model with the results for the liquid-side limited model described in the main text and experimental data. The CO_2 absorption predicted by the liquid-limit model is about two orders of magnitude smaller than predicted by the gas-side model, indicating that liquid-side mass transfer is limiting. The experimental data confirm this.

Calculating CO_2 flux and k_{spray}

This section refers to CO_2 flux, J_{CO_2}, given by Equation 1 in the main text:

$$J_{CO_2} = C K_H \sqrt{D_l k \{OH^-\}}$$

and k_{spray} as defined by Equation 5 of the main text:

$$k_{spray} = J_{CO_2}/C = K_H\sqrt{D_l k\{OH^-\}}$$

Ionic strength and solution viscosity affects each of the parameters in the flux equation. In early work, researchers grouped these effects together with an empirical correction to the rate constant k. However, corrections to each parameter now exist which allow k to remain constant at its dilute value. The basic effects on each parameter at increasing solution concentrations are as follows: (1) the solubility of CO_2 (K_H) decreases with increasing ionic strength, known as a "salting out" effect, (2) the diffusion coefficient decreases due to an increase in solution viscosity, and (3) the activity coefficient of the hydroxide ion is less than 1 up to an ionic strength of about 4 M and then becomes greater than 1. Considering each of these effects, k_{spray} is calculated using the following:

$$k_{spray} = \frac{K_H^\circ}{\gamma_{CO_2}}\sqrt{\frac{D_l^\circ}{\mu^{1.14}}k\gamma_{NaOH}[OH^-]} \quad \text{(SI3)}$$

The rate constant, k, for the elementary reaction:

$$CO_2(aq) + OH^- \longrightarrow HCO_3^-$$

should remain constant for a fixed temperature. Changes in apparent reactivity are attributed to changes in activity of the reacting species. Thus for the base case we have chosen to calculate k_{spray} by assuming a steady rate constant for the reaction of 8500 L mol^{-1}s^{-1}(*5*) and adjusting the Henry's constant following Duan and Sun (*6*), the activity coefficient for OH^-, γ_{NaOH}, using the Pitzer equation and appropriate parameters (*7*), and the effect of solution viscosity on the diffusivity of CO_2 following Hayduk and Laudie (*8*), where D_l° is the diffusivity in a dilute solution and μ is the viscosity of the solution in centipoise. Each of these corrections is described below.

Effect of [NaOH] on K_H

The Henry's constant (i.e. solubility) of CO_2 into the NaOH solution is a function of ionic strength. The effect of ionic strength on K_H is given by:

$$\gamma_{CO_2} = \frac{m_{CO_2}^\circ}{m_{CO_2}}$$

Where $m_{CO_2}^\circ$ is the aqueous solubility of CO_2 in pure water at a specified pressure and temperature and m_{CO_2} is the aqueous solubility of CO_2 in a NaCl solution of a given molality. Gamma is calculated using a Pitzer formulation given by Duan and Sun (*6*), which is a non-linear empirical relationship used to fit solubility data vs. solution composition. γ_{CO_2}monotonically increases from a value of 1.06 at 0.35M NaCl to 1.89 at 5M. The Pitzer parameters cannot be

measured directly for NaOH because of the reaction between CO_2 and OH^-, however, it is reasonable to assume that these values would be similar for NaOH since it is also a 1:1 electrolyte. Given this range, the solubility of CO_2 at the drop surface decreases by up to a factor of 1.9 for an increase in NaOH concentration of 5M compared to a dilute state. We use the value from Stumm and Morgan (*5*) of the dilute-state Henry's constant for 20°C and sea-level pressure.

Effect of [NaOH] on the activity of OH^-

Increasing the ionic strength of a sodium hydroxide solution changes the activity of the dissolved ions in solution. This partly offsets the increase of CO_2 flux into the droplets due to higher [OH^-]. The Pitzer equation is used to calculate the activity coefficient of OH^- in solution (*7*):

$$\ln\gamma_{\mathrm{NaOH}} = -A\frac{I^{0.5}}{1+bI^{0.5}} + \frac{2}{b}(I+bI^{0.5})|Z_M Z_X| + \frac{4V_M V_X}{\nu} m\beta^{\circ}_{MX} + \frac{6(V_M V_X)^{1.5}}{\nu}|Z_M Z_X|^{0.5} m C_{MX}$$

Here, m is the molality of the sodium hydroxide solution, I is the solution ionic strength, and the other parameters are empirically derived for NaOH and can be found in Perex-Villasenor et al. (*7*). Using this equation, the activity coefficient for NaOH decreases from 1 at infinite dilution to a value of 0.6 for NaOH ranging from 0.35M to 1.3M, then increases again reaching a value of 1.3 at 5M. This type of response in typical for charged species in solution such as OH^-. Thus, the maximum effect of ionic strength on CO_2 flux is a decrease to 70% of its value at infinite dilution up to 1.3M NaOH. At 5M the increase in CO_2 flux is 14%. These effects are relatively small compared to the effect on the Henry's constant and the diffusion coefficient.

Effect of ionic strength on D_l

The diffusion coefficient decreases with increasing NaOH concentration due to the increased viscosity of the fluid. The diffusion coefficient is calculated using the method of Hayduk and Laudie (*8*), where μ is the solution viscosity (in centipoises) and V is the molar volume (27.5 $\mathrm{cm^3 mol^{-1}}$ for CO_2):

$$D_l = \frac{13.26\times10^{-5}}{\mu^{1.14}V^{0.589}} = \frac{D_l^{\circ}}{\mu^{1.14}}\ (\mathrm{cm^2 s^{-1}})$$

The NaOH solution viscosity at 20 °C ranges from 1 centipoise at infinite dilution to 2.87 centipoise at 5M, giving a range of diffusion coefficients ranging from 1.88×10^{-6} $\mathrm{cm^2 s^{-1}}$at infinite dilution to 5.67×10^{-7} $\mathrm{cm^2 s^{-1}}$ at 5M. Thus, the diffusion coefficient decreases by roughly a factor of 3 over the range of [NaOH] used, yielding a maximum effect on flux of $\sqrt{3}$ or about 1.7.

Effect of ionic strength on k

The reaction rate constant, k, increases with ionic strength as reported by Astarita (*9*) and by Danckwerts (*10*). Astarita reports an observed increase in k from 5000 $\mathrm{L\,mol^{-1}s^{-1}}$ to 22,300 $\mathrm{L\,mol^{-1}s^{-1}}$ at 5M NaOH. Similarly, Danckwerts reports an increase in k from 6000 $\mathrm{L\,mol^{-1}s^{-1}}$ to 22,000 $\mathrm{L\,mol^{-1}s^{-1}}$ with the addition of 5 M KCl. These are based on empirical relationships from data collected over a range of ionic strengths and incorporate the effects of ionic strength on the Henry's constant, the diffusion coefficient, and the activity of hydroxide ion.

Since it is difficult to separate out each effect from such an empirical relationship, there are two approaches that can be used to calculate J_{CO_2} and hence k_{spray}. The first is to use a fixed value of k and to adjust J_{CO_2} for [NaOH] according to the above relationships for the effect of ionic strength on the Henry's constant, the diffusion coefficient, and the activity coefficient for OH^-. Since, in principle for an elementary reaction k should remain constant this is the approach that we used. We used the value of k reported by Stumm and Morgan (*5*) of 8500 $\mathrm{L\,mol^{-1}s^{-1}}$. Note that in this approach the flux does not increase as rapidly as would be predicted for an increase in $[OH^-]$ alone. This agrees with our experimental values (Figure 3 of the main text). On the other hand, according to Astarita and Danckwerts, the reaction constant, k, is predicted to increase with increasing $[OH^-]$ but the activity of $[OH^-]$ is not adjusted for ionic strength. Both approaches give similar values for the CO_2 absorption in the end but individual factors vary.

Still, there is some uncertainty in the predicted CO_2 flux. We address this by calculating k_{spray} using the approach above and also for low and high bounds of k_{spray}. The low bound is the value implied by our experimental measurements coupled with the coalescence model, giving a value 20% below the theoretical prediction for 1.3 M solution. The high bound is defined by the highest absorption rate calculated from values in the literature, i.e. values from Astarita (*9*) for a 5M solution. We correct the diffusivity for solution viscosity in this calculation, though it is not clear whether Astarita does this. Thus this estimate may be conservative.

All considered, the k_{spray} used in cost calculations amounts to 0.0025 m/s, which correspondes to a 2.5M solution. We chose this molarity because it gives close to the maximum absorption rate with a lower-viscosity (and thus more spray-friendly) solution, and is also in the range of concentrations chosen for previous studies of CO_2 absorption by NaOH solution. In any case, Table 1 shows that variation in k_{spray} between 1.3 and 5M is small.

In our sensitivity analysis, as a lower bound we consider a k_{spray} value in line with our experimental measurements coupled to our coalescence model, 0.0018 m/s, and as an upper bound we consider the highest k_{spray} calculated from values in the literature for a 2.5M solution, which comes from Pohorecki and Wladyslaw (*11*). Table 1 shows parameters used in the calculation of k_{spray} for cost estimates along with comparable values for other NaOH concentrations and from other sources.

Case	k [L mol^{-1}s^{-1}]	[OH$^-$]	γ_{NaOH} []	$K_H \left[\frac{mol/L_{soln}}{mol/L_{air}}\right]$	γ_{CO_2}[]	D_l [m^2/s]	k_{spray} [m/s]
0.33M NaOH	8500	0.33	0.61	0.87	1.06	1.88×10^{-9}	0.0015
1.33M NaOH	8500	1.33	0.59	0.87	1.21	1.53×10^{-9}	0.0023
2.5M NaOH	8500	2.5	0.66	0.87	1.4	1.12×10^{-9}	0.0025
5M NaOH	8500	5.0	1.3	0.87	1.89	5.67×10^{-10}	0.0026
Zeman 1M (*12*)	6745	1.0	1	0.79	1	1.78×10^{-9}	0.0027
Danckwerts 2M (*10*)	6000	2.0	1	0.48	1	1.0×10^{-9}	0.0017
Astarita 2.5M (*9*)	10568	2.5	1	0.61	1	1.12×10^{-9} [a]	0.0030
Pohorecki et al. 2.5M (*11*)	16512[b]	2.5	1	0.60	1	1.09×10^{-9}	0.0040

Table 1: Calculation of k_{spray}: values used in Equation SI3.
[a] It is not clear whether Astarita corrects the diffusivity for viscosity. We have applied our own correction.
[b] Using the fitted formula for CO_2-NaOH.

CO_2 depletion in air

We approximate the spray surface area per unit contactor volume, S, as uniform along the length of the contactor. The concentration of CO_2 in air, C then follows first-order decay, so that Equation 5 in the main text can be integrated to yield:

$$C = C_{in} e^{-S k_{spray} t} \tag{SI4}$$

To get the outlet concentration, C_{out}, we evaluate this at the residence time of air in the contactor, $t = \frac{L}{v_{air}}$ where L is the length of the contactor and v_{air} is the horizontal air velocity:

$$C_{out} = C_{in} e^{-S k_{spray} L / v_{air}} \tag{SI5}$$

We choose the ratio L/v_{air} to give $C_{in} - C_{out} = \Delta C$ high enough that fan energy per unit CO_2 is small, but low enough that CO_2 is not substantially depleted in the outlet air (which would reduce the absorption efficiency of the spray). The average CO_2 concentration in the contactor, C_{avg}, is a function only of ΔC. It can be shown from integration of Equation SI4 that

$$C_{avg} = -\Delta C / \ln(1 - \Delta C / C_{in}) \tag{SI6}$$

For our cost calculations, we choose a CO_2 capture rate from air of 30%, which gives $C_{avg} = 0.84 C_{in}$.

Prototype photographs

The prototype was constructed and tested over the period of June to December, 2005 at the University of Calgary. Figures SI3 and SI4 show photographs of the completed prototype.

Figure SI3: Photograph of completed prototype structure from below.

Figure SI4: Photograph of completed prototype structure from above.

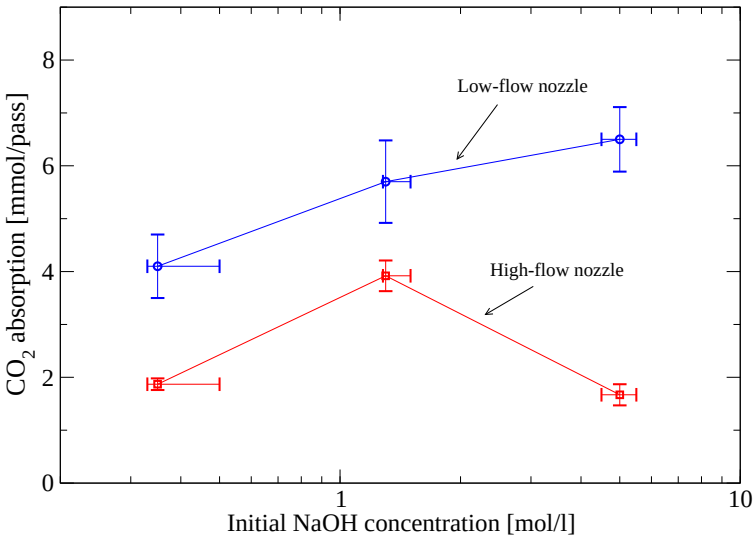

Figure SI5: CO_2 absorption for several solution concentrations of NaOH and two nozzles. Nozzle pressure is held constant. Absorption does not rise as quickly with hydroxide concentration as would be expected in the ideal case.

Sodium hydroxide concentration effect

With other parameters fixed, changing the solution concentration has competing effects. Higher concentration solutions should absorb better due to a faster reaction rate (Equation 3 in the main text), but it is also known that higher viscosity solutions produce larger drops from typical nozzles (*13*). Figure SI5 shows absorption for 3 different NaOH concentrations. For the low-flow nozzle, absorption increases with concentration, but not as quickly as would be expected for sprays of constant drop size. The high flow nozzle peaks with the 1.3 M solution, and the 5 M solution absorbs even less than the 0.33 M solution. The effect of viscosity is highly dependent on nozzle geometry, and this may explain the discrepancy.

Component cost calculations

Here we calculate the costs of the most important non-structural components of the contactor. These results can be viewed as a double-check on the capital cost estimates obtained from industry experts in the main text, which are meant to include all these components.

These calculations can be made without reference to structural form or overall size of the contactor using a few basic assumptions. They include:

- capital charge rate, including operation and maintenance, is 19% per year
- CO_2 capture efficiency from air is 30%
- CO_2 captured per pass is 9 mmol per L of solution, matching the base case model result at a 10 L/min flow rate.

Taking the retail price of the high-flow nozzle used in the prototype (*14*), the nozzle cost comes to 4 \$/ton-CO_2. This is a stainless steel nozzle, and the the same model nozzle made of polyvinyl chloride (PVC), which should also be compatible with NaOH solution, would be 1 \$/ton. A lower solution flowrate, putting the contactor in a more energy-efficient regime, as discussed in the main text, would reduce the nozzle cost as well.

Capital and installation cost for pumps was obtained from the GTPro / PEACE software for power plant cooling tower design and cost estimation (*15*). The resulting 2 \$/ton-CO_2 is sensitive to solution flowrate (and lower for lower flowrates) as discussed for the nozzles.

There are many options for the particle trap that sits at the outlet of the contactor collecting small drops entrained in the outlet air. We obtained a cost quote for one model of wire-mesh trap that provides high collection efficiency with a low pressure drop. If the trap area is equal to the vertical cross-sectional area of the contactor, this comes to 7 \$/ton-CO_2. However, one could construct the contactor with a constricted outlet area – perhaps half or less of the cross-sectional area, which would reduce the trap cost proportionally. Higher air-flow rates would reduce the trap cost per ton CO_2, but may increase the pressure drop (and thus fan energy). This calculation is based on a small-order price (only several m^2 of trap area), and presumably a large bulk order would be significantly less expensive.

Considering high-volume order discounts and ability of the designers of a full-scale contactor to seek inexpensive components, it seems the cost of nozzles, pumps, and the particle trap will be small compared to overall capital cost.

References

(1) Adams, T. N. Lime Reburning. In , Vol. 1. 5 Alkaline Pulping; Joint Textbook Committee of the Paper Industry: 1989; Chapter XXII, pages 590–608.

(2) Keith, D.; Ha-Duong, M.; Stolaroff, J. K. Climate strategy with CO_2 capture from the air. *Climatic Change* **2006,** *74,* 17–45.

(3) Seinfeld, J. H.; Pandis, S. N. *Atmospheric Chemistry and Physics;* John Wiley and Sons: New York, 1998.

(4) Bird, R.; Stewart, W. E.; Lightfoot, E. N. *Transport Phenomena;* John Wiley and Sons: New York, 1960.

(5) Stumm, W.; Morgan, J. *Aquatic Chemistry;* John Wiley & Sons, Inc.: New York, 1996.

(6) Duan, Z.; Sun, R. An improved model calculating CO2 solubility in pure water and aqueous NaCl solutions from 273 to 533 K and from 0 to 2000 bar. *Chemical Geology* **2003,** *193,* 257–271.

(7) Perez-Villasenor, F.; Iglesias-Silva, G.; Hall, K. Osmotic and Activity Coefficients Using a Modified Pitzer Equation for Strong Electrolytes 1:1 and 1:2 at 298.15 K. *Industrial & Engineering Chemistry Research* **2002,** *41,* 1031-1037.

(8) Hayduk, W.; Laudie, H. Prediction of Diffusion Coefficients for non-electrolytes in dilute aqueous solutions.. *J. AIChE* **1974,** *20,* 611–615.

(9) Astarita, G. *Mass Transfer with Chemical Reaction;* Elsevier: Amsterdam, 1967.

(10) Danckwerts, P. V. *Gas-Liquid Reactions;* McGraw-Hill: New York, 1970.

(11) Poherecki, R.; Moniuk, W. Kinetics of reaction between carbon dioxide and hydroxly ions in aqueous electrolyte solutions. *Chemical Engineering Science* **1988,** *43,* 1677–1684.

(12) Zeman, F. Energy and Material Balance of CO2 Capture from Ambient Air. *Environmental Science and Technology* **2007,** ASAP Online.

(13) Lefebvre, A. H. *Atomization and Sprays;* Taylor and Francis: 1989.

(14) Allspray, "Online Catalog", Technical Report, Allspray Inc., 2007 Available: http://www.allspray.com.

(15) Thermoflow, "GTPRO/PEACE v. 16", 2006.